Title
Cytomegalovirus Immediate-Early Proteins Promote Stemness Properties in Glioblastoma

Journal
Cancer Research, 75(15)

ISSN
0008-5472

Authors
Soroceanu, Liliana
Matlaf, Lisa
Khan, Sabeena
et al.

Publication Date
2015-08-01

DOI
10.1158/0008-5472.can-14-3307

Peer reviewed

HHS Public Access

Author manuscript

Cancer Res. Author manuscript; available in PMC 2016 August 01.

Published in final edited form as:

Cancer Res. 2015 August 1; 75(15): 3065–3076. doi:10.1158/0008-5472.CAN-14-3307.

Cytomegalovirus immediate early proteins promote stemness properties in glioblastoma

Liliana Soroceanu[a,1], **Lisa Matlaf**[a], **Sabeena Khan**[a], **Armin Akhavan**[a], **Eric Singer**[a], **Vladimir Bezrookove**[a], **Stacy Decker**[b], **Saleena Ghanny**[c], **Piotr Hadaczek**[d], **Henrik Bengtsson**[e], **John Ohlfest**[b], **Maria-Gloria Luciani-Torres**[a], **Lualhati Harkins**[f], **Arie Perry**[g], **Hong Guo**[c], **Patricia Soteropoulos**[c], and **Charles S Cobbs**[d,h,1]

[a]Department of Neurosciences, California Pacific Medical Center Research Institute, 475 Brannan Street, Suite 220, San Francisco, CA, 94107

[b]Department of Pediatrics and Neurosurgery, University of Minnesota Masonic Cancer Center, Minneapolis, MN, 55455

[c]Center for Applied Genomics, Institute of Genomic Medicine UMDNJ-New Jersey, 225 Warren Street Newark, NJ 07103

[d]Department of Neurological Surgery, University of California, San Francisco, 400 Parnassus Avenue, San Francisco, CA 94102

[e]Department of Epidemiology and Biostatistics, University of California, San Francisco, CA, 94158

[f]Department of Pathology, University of Alabama at Birmingham, 619 South 19th Ave, Birmingham, AL, 35233

[g]Department of Pathology, University of California, 505 Parnassus Avenue, San Francisco, CA, 94143

[h]Ben and Catherine Ivy Center for Advanced Brain Tumor Treatment, 550 17th Avenue, Suite 540, Seattle, WA 98122

Abstract

Glioblastoma (GBM) is the most common and aggressive human brain tumor. Human cytomegalovirus (HCMV) immediate early (IE) proteins that are endogenously expressed in GBM cells are strong viral transactivators with onconcogenic properties. Here, we show how HCMV IE are preferentially expressed in glioma stem-like cells (GSC), where they co-localize with the other GBM stemness markers, CD133, Nestin, and Sox2. In patient-derived GSC that are endogenously infected with HCMV, attenuating IE expression by an RNA-i-based strategy, was sufficient to

[1]Corresponding authors: Liliana Soroceanu, CPMC Research Institute, 475 Brannan Street, Suite 220, San Francisco, CA, 94107, Phone: +1 415 600-1770, Fax: + 1 415 600-1725, sorocel@cpmcri.org and Charles Cobbs: charles.cobbs@gmail.com.

Author Contributions L.S., L.M, S.K., S.D., J.O., M.G.L.T., A.A., S.G., and H.G. performed experimental work. A.P. scored mouse glioma tissues (blinded to experimental details). L.S., H.B., E.S., D.M., S.G., and P.S. performed data analysis. L. S., L.M., H.B., D.M, and E.S. produced the figures. C.S.C. provided patient material. L.S. and C.S.C conceived and wrote the manuscript. All authors contributed to the final manuscript.

The authors declare no conflict of interest.

inhibit tumorsphere formation, Sox2 expression, cell cycle progression, and cell survival. Conversely, HCMV infection of HMCV-negative GSC elicited robust self-renewal and proliferation of cells that could be partially reversed by IE attenuation. In HCMV-positive GSC, IE attenuation induced a molecular program characterized by enhanced expression of mesenchymal markers and pro-inflammatory cytokines, resembling the therapeutically-resistant GBM phenotype. Mechanistically, HCMV/IE regulation of Sox2 occurred via inhibition of miRNA-145, a negative regulator of Sox2 protein expression. In a spontaneous mouse model of glioma, ectopic expression of the IE1 gene (*UL123*) specifically increased Sox2 and Nestin levels in the IE1-positive tumors, upregulating stemness and proliferation markers in vivo. Similarly, human GSC infected with the HCMV strain Towne but not the IE1-deficient strain CR208 showed enhanced growth as tumorspheres and intracranial tumor xenografts, compared to mock-infected human GSC. Overall, our findings offer new mechanistic insights into how HCMV/IE control stemness properties in glioblastoma cells.

Keywords

Glioblastoma; HCMV; IE1; Cancer Stem Cells; Sox2; mir-145; gliomagenesis

INTRODUCTION

Human cytomegalovirus (HCMV), a neurotropic beta-herpes virus, is the most common cause of congenital brain infection. HCMV gene expression in the developing brain interferes with the proliferation and differentiation of neural precursor cells (NPC), often causing severe brain injury (1). We and others detected HCMV infection and expression of its immediate early gene (IE) products in a high percentage of human glioblastomas (GBM) (2–4), and subsequently showed that IE1 expression increased GBM proliferation by modulating the activity of key oncogenic signaling pathways (5). Both IE1 (IE72) and IE2 (IE86) proteins- collectively referred herein as HCMV IE- have mutagenic properties, interfere with the function of p53 and Rb tumor suppressors, promote the S phase and inhibit apoptosis of infected cells (6–10). Glioblastoma stem-like cells, characterized by tumor initiating potential in vivo and expression of stemness markers, have been shown to endow GBM tumors with resistance to therapy and drive tumor recurrence (11–14). GSCs lack DNA repair mechanisms(15), which maintain herpes viruses in a latent state in normal neural stem cells (16), rendering these cells ideal hosts for persistent HCMV infection and/or reactivation. Given the critical role of GSC in glioma pathogenesis and the observation that HCMV IE levels in endogenously infected GBMs negatively correlate with patient outcome (17), we set out to investigate the role of HCMV IE in the growth and survival of GSC using clinically relevant culture and mouse models of primary GBM. Our results demonstrate a novel role for HCMV IE, as potent drivers of GSC.

MATERIALS AND METHODS

Ethics statement

All human samples were obtained with informed consent after approval of the Institutional Review Board of CPMC hospital. All animal studies were conducted using institutional IACUC approved protocols.

Data availability

Data obtained using Affymetrix and HCM VDNA arrays was analyzed as described (18,19). Human, mouse, and HCMV microarray data are available under GEO submission **GSE 56752**.

Glioblastoma Primary cultures

Primary glioblastoma cultures were generated using tissue from surgical resections at CPMC obtained according to the IRB approved protocol. For each GBM primary lines, a pathology report accompanying the corresponding tissue of origin confirmed the identity of the primary cells. In addition, matched blood was collected from the same patients for serology analyses. Tissues were dissociated using enzymatic and mechanical dissociation as previously described (20). CD133 and SSEA1 positive and negative fractions were obtained by magnetic activated cell sorting (MACS), using the autoMACS Pro Separator in conjunction with cell separation reagents from Miltenyi Biotec (kit #130-050-801 for CD133, kit # 130-094-530 for SSEA1, and # 130-090-101 dead cell removal kit). Single cell suspensions were cultured using neural basal medium+ N2 supplement, 20 ng/ml EGF, 20 ng/ml bFGF, and 1μg/ml laminin as previously described (21). All acutely dissociated cells were used within 3–5 passages. Primary GSC lines obtained from Dr. Jeremy Rich's laboratory were authenticated using the Promega cell line authentication service and maintained in our laboratory 4–6 months by serial in vivo passaging. All human primary GBM cells tested negative for Mycoplasma, using R&D "Microprobe", catalog # CUL001B kit.

GSC self renewal assays

Where indicated, GSC derived from mouse xenografts were resorted for CD133 (lines with proneural molecular profile) or CD44 (lines with mesenchymal molecular profile) prior to functional studies, as previously described (22). The cancer stem cell phenotype of GSCs was validated by functional assays of self-renewal (serial neurosphere passage), and tumor propagation (in vivo limiting dilution assay). To generate single GSC-derived tumorspheres, the sorted GSCs were seeded in 96-well plates by serial dilution or by the FACS sorter. The single GSC-generated neurosphere from each well was transferred into new well of a 24 well plate for secondary sphere assays. The freshly sorted GSCs from GBM surgical specimens or xenografts and the derived GSC tumorspheres were used for in vitro or in vivo experiments as indicated. U87 glioma and HEL cell lines were obtained from ATCC and maintained in DMEM+10% FBS. ATCC cell line authentication data for these two lines.

Spontaneous Mouse Glioma Model

Balb/c mice were bred and handled according the Institutional Animal Care and Use Committee protocol. The intracerebral ventricular method of injection has been described previously (33). Postnatal day one mice were anesthetized using hypothermia and placed on a cooled stereotaxic neonatal frame. In vivo jetPEI^{TM} (Polyplus^{TM}) mixed with plasmid DNA (700ng total DNA) was injected at a flow rate of 0.4μl/min into the right lateral ventricle. The following plasmids were utilized for glioma induction in equal parts: pT2/C-Luc/PGK-SB100, pT2/Cag-NrasV12, pT2/shP53/GFP4/mPDGF, and pT2/Cag-IE1 or pT2/C-Neo. Tumor development was monitored starting at three weeks of age by *in vivo* bioluminescence. At moribund stage, animals were anesthetized with a ketamine/xylazine cocktail and transcardially perfused with phosphate buffered solution followed by 4% paraformaldehyde. Brains were collected and post-fixed in 10% formalin. Alternatively, brains were collected without perfusion, snap frozen in a dry ice-ethanol bath, and shipped on dry ice. Freshly harvested mouse tissue was handled the same way as human tissue for generation of mouse glioma neurospheres.

Viability of GSC was measured using Cell Titer-GLO Luminescent Cell Viability Assay (Promega). Data shown is representative of an $n \geq 6$ for all data points, and all data analysis was performed using GraphPad Prism.

Data analysis and statistical procedures

All data shown represents two independent experiments with ≥ 3 replicates. The IC_{50} values with corresponding 95% confidence limits were compared by analysis of logged data (Graph-Pad Prism). Significant differences were also determined using a one-way ANOVA or the unpaired Student's t-test, where suitable.

Additional Methods are detailed in the Supplementary Information file linked to this manuscript.

RESULTS

HCMV IE and markers of glioblastoma stemness are co-expressed in situ

Acutely dissociated primary patient-derived GBM cells (four samples were tested, Table S1) were used to investigate the extent to which IE expression is enriched in the CD133+ tumor cell subpopulation using fluorescence activated cell sorting (FACS) of doubly labeled cells. CD133 is an antigen enriched in GSC and routinely used for analysis of primary GBM samples (12). Over 70% of IE positive cells were also CD133+ with the fraction of double positive cells between 1.2–8.2% among the tested samples (Figure 1A, Table S1). Using RT-PCR we screened ten flash-frozen GBM tissue samples for expression of HCMV IE; we detected IE1 mRNA in over 75% and IE2 in ~30% of GBM samples, but not in control, non-tumor samples (Figure 1B and Table S1). RT-PCR products were sequenced to exclude the possibility of laboratory HCMV contamination (Figure S1). We next compared CD133 positive and negative cell fractions from three fresh GBM samples for the presence of IE1 using RT-PCR (n=6) and western blot (n=4). MAB810 (from Chemicon) which recognizes both IE1 and IE2 was used for immunofluorescence and western blot analyses, therefore we

will refer to the antigen detected using this antibody as HCMV IE. Representative examples shown in Fig 1C–E, demonstrate that IE1 levels are enriched in the CD133+ positive cell fraction in two acutely dissociated GBM cultures (CPMC-085, CPMC-099). IE1 (exon 4) transcript and IE proteins were specifically detected in the CD133+ fraction (Fig 1C). We screened additional primary GBM samples, using a different glioma stem cell marker, the stage specific embryonic antigen 1 (SSEA1 or CD15). Taqman analysis of positive and negative fractions, showed that IE1 expression was enriched in the SSEA1+ subpopulation compared to the negative fraction by 2.1 and 5.9 fold respectively in two patient samples (Figure S2).

Next, we used matched tissue and primary cultured cells from three GBM cases to interrogate IE localization *in situ*. CPMC-041 tissue was processed to generate subcellular fractions; we found IE expressed in the nuclear and cytoplasmic compartments (Figure 1F), which is a pattern distinct from that described in lytic infection of fibroblasts (23). Freshly isolated, CD133+ cells from the same tissue sample (CPMC-041) were grown as neurospheres and processed by double immunofluorescence. Figure 1G demonstrates co-localization of IE with Nestin in the endogenously HCMV-infected neurospheres. CPMC-085 matched tissue and cells demonstrated co-localization of SOX2 and IE (Figure 1H, I). Double immunofluorescence analyses of CPMC-099 tissue and cells showed co-localization of HCMV IE with Nestin (Figure 1J) and Sox2 (Figure 1K), both markers associated with glioma stem-like phenotype (24). Quantification of double positive cells was performed by counting 6 low magnification microscopic fields in each of the three samples. Average number of double positive cells was compared to total number of cells examined; results showed that between 38–45% tumor cells positive for both Nestin and IE and 50–60% cells were immunopositive for both IE and Sox2. Using freshly isolated primary cells isolated from a distinct GBM sample, we found IE co-localized with PDGFRα, Integrin α6, and Olig2 (Figure S2B–E), all of which are enriched in various subsets of glioma stem-like cells (25–27). A summary of viral and cellular proteins detected in forty human brain tissue samples is shown in Table S1. We also interrogated the *CMV serostatus* in a subset of patient plasma samples using a clinical grade ELISA kit. Results indicate that in ~ 40% of GBM cases, CMV specific IgG or IgM were detectable in peripheral blood (supplementary Table S2). The absence of circulating antibodies in some cases with IE1+ tumor tissues may be attributed to overall immune anergy of GBM patients or the assay's sensitivity limit.

HCMV IE regulate GSC by modulating the mi-RNA145-Sox2 axis

Given the strong association with GSC markers in primary-derived GBM tissues and cells, we set out to investigate whether HCMV IE is actively involved in regulating the cancer stem-like phenotype. To test this hypothesis, we used a combination of two siRNA duplexes to knockdown (KD) IE in HCMV-positive GSC samples. When used together, these siRNA duplexes target exons 3 and 4 of the *UL123* gene (28), inhibiting expression of both IE1 and IE2 proteins. We chose the combination of two siRNA sequences for functional studies, since the extent of protein KD and subsequent effects on proliferation and self-renewal of HCMV positive GSC were more potent than using either sequence alone (Figure 2A, Figures S3-S4). Henceforth, the term IE siRNA designates the use of two combined siRNA sequences, targeting both IE1 and IE2; the term IEKD refers to IE1/IE2 protein knockdown.

Mechanistic studies presented here were performed using two endogenously HCMV-infected, acutely dissociated GBM samples (CPMC-085 and CPMC-099) and three pre-established GSC lines, initially HCMV negative. Treatment with IE siRNA of CD133+ cells from CPMC-085 and CPMC-099 caused significant reduction in the number of neurospheres (Figure 2B). Self-renewal assays showed that IEKD inhibited both primary and secondary neurosphere growth by ~ 50–60% (Figure 2C). Conversely, HCMV infection of HCMV-negative GSC4121 promoted self-renewal, which was partially reverted by IEKD (Figure S3). The knockdown effect was specific, since uninfected cells were not impacted by IEKD (Figure S3). Limited dilution assays of HCMV infected GSC4121 and GSC0609 show a significant decrease in glioma stem cell frequency in the IEKD compared to control conditions (Figure S4).

We investigated the mechanism underlying HCMV regulation of GSC self-renewal by screening a human stem cell antibody array followed by western blot validation. As shown in Figure 2D and Figure S5, IEKD in CD133+cells isolated from CPMC-099 and CPMC-085 inhibited expression levels of several stem cell markers, particularly Sox2, an essential regulator of GBM initiation and growth (29). We have previously identified a number of microRNAs modulated by HCMV in human neural precursor cells (unpublished results), including micro RNA 145 (miR-145). miR-145 is a potent negative regulator of Sox2 expression in human embryonic stem and glioma cell lines (30,31). Using Taqman specific for miR-145, we determined that HCMV infection of three GSCs (initially HCMV negative) induced a 2.5–2.7fold decrease in miR-145 levels (Figure 2E). This effect was partially reverted by pretreatment with the mature miR-145 mimic prior to HCMV infection of GSC. Importantly, HMCV infection followed by IEKD also attenuated virus-induced inhibition of miR-145 levels, suggesting that HCMV IE play a major role in modulating the miR-145-Sox2 axis (Figure 2E). In the converse experiment we over-expressed the HCMV *IE1* gene in GSC4121 and found that IE1 inhibits miR-145 and simultaneously upregulates Sox2 protein, albeit to a lesser extent than the whole virus (Figure S6).

To demonstrate specificity, we used both knockdown and overexpression of miR-145. We found that HCMV-induced Sox2 and Oct4 protein increases were partially reverted by over-expression of miR145 in GSC4121 (Figure 2F). Furthermore, HCMV-induction of tumorsphere growth in all three GSC lines was partially inhibited by pretreatment with HSA-miR-145 (Figure 2G). Mechanistically, we propose that HCMV infection of GSC inhibits miR-145 expression, which in turn relieves negative regulation of Sox2 protein and this effect is driven in part by HCMV IE1 protein (Figure 2H).

IEKD inhibits cell cycle progression of HCMV positive GSC

Since Sox2 KD had been shown to inhibit GBM growth by regulating GSC proliferative capacity (29), we investigated how IEKD impacts cell cycle progression in four primary GBM-derived cultures, positive for HCMV. Using BrdU incorporation in conjunction with flow cytometry, we determined that IEKD reduced the percentage of cells in S-phase between 12–39% (Figure 3A–B). Western blot analysis of one of the samples showed that mechanistically IEKD inhibits TOP2A expression, which is consistent with a decrease in cell proliferation (Figure 3C).

IE knockdown induces apoptosis of HCMV positive GSC

To more accurately assess the consequences of HCMV infection on GSC survival we assessed tumorsphere growth using the CD133+ cell fraction from three GSC lines (4121, 0609, 3832), infected with HCMV and treated with control or IE siRNA. HCMV potently increased tumorsphere growth and this effect was significantly inhibited by IEKD (Figure 4A–B). Using Cell Titer Glo assay, we found that IEKD significantly inhibited cell viability of HCMV-infected GSC4121 (Figure 4C). Primary GBM cells from three GSC lines and two fresh GBM samples were used to assess apoptosis, using Apo-BrdU staining in conjunction with flow cytometry. IEKD induced apoptotic cell death specifically in HCMV infected GSC (Figure 4D). Taken together, these results reveal an important anti-apoptotic role for IE1 in HCMV infected GSC, as it has been reported in other cell systems (32–34).

To interrogate the molecular mechanisms underlying GSC apoptosis, we used an antibody array which revealed that, in HCMV-positive GSC, the p53 and Caspase3 pathways were activated by IEKD (Figure 5A–B). Interestingly, we also found that Bax was upregulated by IEKD. During lytic infection cycle in fibroblasts, Bax is inhibited by the HCMV anti-apoptotic protein UL37, which ensures cellular death does not preclude new virus production (35). Western blot analyses corroborated these findings (Figure 5B), suggesting that additional viral genes and their cellular signaling partners are impacted by the IE knockdown.

IEKD induces a mesenchymal and proinflammatory phenotypic shift in HCMV positive GSC

Following IEKD of HCMV-infected GSC, we noticed a subset of tumorspheres survived treatment and continued to grow. To investigate specific pathways which drive the survival of this “resistant” subpopulation, we sorted live cells seven days following IEKD and performed transcriptome profiling using both HCMV and human Affymetrix DNA arrays. Statistical analysis of microarray (SAM) data revealed a large number of viral transcripts significantly downregulated by IEKD (Figure 5C and associated microarray data), including viral Interleukin-like 10, previously shown to enhance the immunosuppressive phenotype of human GSC (36). Among cellular gene products, significant downregulation of stemness markers ASCL1, DCX, and PDGFRA was noted (Figure S7 and associated microarray data). Interestingly, a number of cellular transcripts significantly *upregulated* by IEKD were assigned to the mesenchymal and pro-inflammatory functional clusters by the Ingenuity Pathway Analysis (IPA) (Figure S7). We validated these results at the protein level, using a cytokine antibody array (Figure 5D) and western blot analyses (Figure 5E). Our data show that IFNγ, CXCL8, CXCL10 cytokine levels and the GBM mesenchymal marker c-MET were upregulated in the IEKD cells compared to control, while the GBM stemness regulator ASCL1 was downregulated in IEKD cells compared to control (Figure 5D, E).

HCMV *UL123 (IE1)* enhances stemness of spontaneous mouse gliomas

To directly investigate whether the *IE1* gene modulates glioma stem cells *in vivo*, we employed a spontaneous mouse model of disease, which combines knockdown of the p53 tumor suppressor protein with overexpression of *PDGF* and *N-RasV12* oncogenes in the developing neural stem cells (37). Twenty four neonatal mice (three repeat experiments/ two

groups each) were intra-cranially injected with different oncogene combinations +/− *IE1* (Table S3). Tumor penetrance was similar across the two experimental groups, with 20% more GBM tumors developing in the IE1+ experimental group (Table S3). Five weeks following oncogene administration, approximately 75% of mice developed high grade gliomas, exhibiting all pathognomonic features of the disease. An increased number of high grade tumors occurred in the IE1+ group (Figure S8), which is consistent with a previous report showing that HCMV infection at birth can increase tumor aggressiveness in a transgenic mouse model of GBM (38). A neuropathologist "blinded" to the experimental design identified a "giant cell glioblastoma" phenotype specifically in the IE1+ tumors (Table S3). We used this mouse model of glioma to interrogate expression levels of proliferation and stemness markers. Imunohistochemical analysis of matched (+/−IE1) samples showed significant increases in levels of Sox2 (Figure S8) and Nestin, concomitant with a decrease in GFAP levels in IE1-positive compared to control mouse gliomas (Figure 6A–D). Using freshly dissociated mouse brain tissues, we assayed tumorsphere growth in IE1-expressing and control mouse gliomas. Our data show that IE1-expressing cells produced more tumorspheres compared to control mouse glioma cells (Figure 6E). RNA extracted from a subset of mouse tumors was profiled using Affymetrix arrays. Statistical analysis of microarray revealed that IE1-positive tumors clustered together, and segregated away from the controls (Figure 7A). Statistically significant differences in gene expression from several functional categories, including embryonic development, cell cycle, DNA repair, and cell death were measured between IE1- expressing and control mouse gliomas (Figure 7A–C). These cellular processes have been shown to be "hijacked" by IE1 during HCMV infection of various cell types (6). Among the significantly altered transcripts *POU5F1* (Oct 4) and Aurora B kinase (AurBK) were increased (>2 fold) in the IE1 positive mouse gliomas compared to control (Figure 7C and associated microarray data). Imunohistochemical analyses confirmed that upregulation in transcript levels were paralleled by corresponding protein increases for Oct4 and AurBK, in the IE1+ gliomas (Figure 7D–E). Interestingly, in human glioma patients, *p53* mutations cooperate with Aurora B kinase activation in driving giant cell glioblastoma (39), a phenotype we found uniquely associated with the IE1+ mouse gliomas (Table S3). These data indicate that HCMV IE1 expression in the context of pre-existing genetic alterations significantly augmented the glioma stem-like phenotype *in vivo*.

IE1 deficient HCMV, CR208, does not promote GBM stemness as does the parental (Towne) strain

To better understand the specific role that IE1 plays in GSC biology, we utilized an *IE1* deficient HCMV variant (CR208, a gift from Dr. E. Mocarski) and the parental strain (Towne) to infect a GSC culture, initially HCMV negative. While all three GSC lines utilized in this study are tumorigenic in vivo (Figure S9), GSC3832 exhibited most consistent tumor initiation rates in nude mice and was selected for subsequent studies. We monitored neurosphere formation and in vivo growth in mock-, Towne- and CR208-infected, luciferase labeled GSC3832 cells. As shown in Figure S10, CR208 did not significantly induce Sox2 levels and only moderately enhanced tumorsphere formation compared to mock-treated cultures. In contrast, Towne induced significant tumorsphere growth and upregulated Sox2 levels compared to mock conditions. In vivo, Sox2 levels were

elevated in the Towne-infected xenografts, compared to mock or CR208 tumors (Figure S10). Since these GSC are highly tumorigenic at very low cell number (15), we were unable to measure significant differences in tumor initiation rates across the three groups, however Towne-infected GSC-derived tumors exhibited a faster growth rate compared to either Mock, or CR-208 as shown by luminescence measurements (Figure S10). Taken together, our in vivo studies suggest that HCMV *UL123* (IE1) is an important regulator of glioblastoma stem-like phenotype.

DISCUSSION

HCMV impacts oncogenic signaling pathways at multiple levels, by activating receptor tyrosine kinases which drive gliomagenesis, such as PDGFRα (25,40), by promoting the PI3K-AKT-Src pathways (41), inducing an immunosuppressive environment, and by enhancing tumor-promoting “hubs”, such as p-STAT3 (42). Data presented herein demonstrate novel mechanisms by which HCMV and specifically IE1 promote GBM stemness, cell cycle progression and survival. In patient-derived primary GBM cultures, IEKD significantly altered self-renewal and survival of GSC, suggesting that these HCMV positive glioma cells could be effectively targeted by IEKD. Following IEKD, a subpopulation of HCMV positive GSC shifted toward a mesenchymal and pro-inflammatory molecular phenotype reminiscent of therapeutically resistant GBM, induced by radiation or anti-angiogenic therapy (43–45). This finding is particularly interesting in light of a very recent study reporting clinical efficacy of a dendritic cell vaccine targeting another HCMV protein (pp65) in GBM patients (46). Our results suggest that immunotherapies aimed at co-targeting multiple HCMV antigens may offer additional therapeutic benefit for HCMV positive glioma patients.

Previous studies have shown that CMV infection in the mouse lead to persistent IE expression in the nestin positive NPC, which continue to self-renew postnatally (47,48). Using a transgenic mouse model of disease, we demonstrate that HCMV *IE1* expression in the context of pre-existing genetic alterations significantly augmented the glioma stem-like phenotype *in vivo*, in agreement with the recent demonstration that mouse CMV can enhance the aggressiveness of murine glioma, when administered neonatally (38). Mouse xenograft studies did not show a difference in tumor initiation, however, HCMV-infected GSC grew at a faster rate in vivo compared to mock, or CR208 (an IE1 deficient virus) infected cells.

Given the fact that *four* current clinical trials are evaluating CMV-specific immunotherapy for GBM patients(49)it is imperative that we better understand the role of the virus in GBM pathogenesis. Data presented here sheds new insights into the role of the virus in regulating genetic and epigenetic networks which promote the growth of cancer stem cells and suggest that targeting IE in HCMV-positive GBMs may have therapeutic benefits by selectively eliminating the cancer stem cell pool.

Supplementary Material

Refer to Web version on PubMed Central for supplementary material.

Acknowledgments

This work was supported by grants NIH R01NS070289 to C.S.C. and LS, NIH R21NS067395 to L.S., ACS research scholar award to C.S.C, and funds from the ABC2 foundation and Flaming foundation. We thank Dr. Victor Goldmacher (Immunogen Inc) for kindly providing the UL37 antibody. We thank Dr. Gregory Riggins (John Hopkins University) and Dr. Jeremy Rich (Cleveland Clinic) for providing GSC lines and Dr. Mark Prichard (UAB) for providing Taqman primers and probes. We are grateful to Dr. Eain Murphy for the IE2 specific antibody and to Dr. Ed Mocarski for the CR208 virus. We thank Dr. Bill Britt for the IE1 exon 4 antibody.

References

1. Cheeran MC, Lokensgard JR, Schleiss MR. Neuropathogenesis of congenital cytomegalovirus infection: disease mechanisms and prospects for intervention. Clin Microbiol Rev. 2009; 22(1):99–126. Table of Contents. [PubMed: 19136436]
2. Cobbs CS, Harkins L, Samanta M, Gillespie GY, Bharara S, King PH, et al. Human cytomegalovirus infection and expression in human malignant glioma. Cancer Res. 2002; 62(12): 3347–50. [PubMed: 12067971]
3. Ranganathan P, Clark PA, Kuo JS, Salamat MS, Kalejta RF. Significant association of multiple human cytomegalovirus genomic Loci with glioblastoma multiforme samples. J Virol. 2011; 86(2): 854–64. [PubMed: 22090104]
4. Scheurer ME, Bondy ML, Aldape KD, Albrecht T, El-Zein R. Detection of human cytomegalovirus in different histological types of gliomas. Acta Neuropathol. 2008; 116(1):79–86. [PubMed: 18351367]
5. Cobbs CS, Soroceanu L, Denham S, Zhang W, Kraus MH. Modulation of oncogenic phenotype in human glioma cells by cytomegalovirus IE1-mediated mitogenicity. Cancer Res. 2008; 68(3):724–30. [PubMed: 18245472]
6. Castillo JP, Yurochko AD, Kowalik TF. Role of human cytomegalovirus immediate-early proteins in cell growth control. J Virol. 2000; 74(17):8028–37. [PubMed: 10933712]
7. Fortunato EA, Sommer MH, Yoder K, Spector DH. Identification of domains within the human cytomegalovirus major immediate-early 86-kilodalton protein and the retinoblastoma protein required for physical and functional interaction with each other. J Virol. 1997; 71(11):8176–85. [PubMed: 9343168]
8. Fortunato EA, Spector DH. p53 and RPA are sequestered in viral replication centers in the nuclei of cells infected with human cytomegalovirus. J Virol. 1998; 72(3):2033–9. [PubMed: 9499057]
9. Hagemeier C, Walker SM, Sissons PJ, Sinclair JH. The 72K IE1 and 80K IE2 proteins of human cytomegalovirus independently trans-activate the c-fos, c-myc and hsp70 promoters via basal promoter elements. J Gen Virol. 1992; 73(Pt 9):2385–93. [PubMed: 1328493]
10. Shen Y, Zhu H, Shenk T. Human cytomagalovirus IE1 and IE2 proteins are mutagenic and mediate “hit-and-run” oncogenic transformation in cooperation with the adenovirus E1A proteins. Proc Natl Acad Sci U S A. 1997; 94(7):3341–5. [PubMed: 9096395]
11. Bao S, Wu Q, Li Z, Sathornsumetee S, Wang H, McLendon RE, et al. Targeting cancer stem cells through L1CAM suppresses glioma growth. Cancer Res. 2008; 68(15):6043–8. [PubMed: 18676824]
12. Fine HA. Glioma stem cells: not all created equal. Cancer Cell. 2009; 15(4):247–9. [PubMed: 19345322]
13. Dirks PB. Brain tumor stem cells: bringing order to the chaos of brain cancer. J Clin Oncol. 2008; 26(17):2916–24. [PubMed: 18539973]
14. Dirks PB. Cancer: stem cells and brain tumours. Nature. 2006; 444(7120):687–8. [PubMed: 17151644]
15. Bao S, Wu Q, McLendon RE, Hao Y, Shi Q, Hjelmeland AB, et al. Glioma stem cells promote radioresistance by preferential activation of the DNA damage response. Nature. 2006; 444(7120): 756–60. [PubMed: 17051156]
16. Luo MH, Rosenke K, Czornak K, Fortunato EA. Human cytomegalovirus disrupts both ataxia telangiectasia mutated protein (ATM)- and ATM-Rad3-related kinase-mediated DNA damage responses during lytic infection. J Virol. 2007; 81(4):1934–50. [PubMed: 17151099]

17. Soderberg-Naucler C. HCMV microinfections in inflammatory diseases and cancer. J Clin Virol. 2008; 41(3):218–23. [PubMed: 18164235]
18. Bengtsson H, Irizarry R, Carvalho B, Speed TP. Estimation and assessment of raw copy numbers at the single locus level. Bioinformatics. 2008; 24(6):759–67. [PubMed: 18204055]
19. Irizarry RA, Hobbs B, Collin F, Beazer-Barclay YD, Antonellis KJ, Scherf U, et al. Exploration, normalization, and summaries of high density oligonucleotide array probe level data. Biostatistics. 2003; 4(2):249–64. [PubMed: 12925520]
20. Soroceanu L, Kharbanda S, Chen R, Soriano RH, Aldape K, Misra A, et al. Identification of IGF2 signaling through phosphoinositide-3-kinase regulatory subunit 3 as a growth-promoting axis in glioblastoma. Proc Natl Acad Sci U S A. 2007; 104(9):3466–71. [PubMed: 17360667]
21. Soroceanu L, Matlaf L, Bezrookove V, Harkins L, Martinez R, Greene M, et al. Human cytomegalovirus US28 found in glioblastoma promotes an invasive and angiogenic phenotype. Cancer Res. 2011; 71(21):6643–53. [PubMed: 21900396]
22. Matlaf LA, Harkins LE, Bezrookove V, Cobbs CS, Soroceanu L. Cytomegalovirus pp71 protein is expressed in human glioblastoma and promotes pro-angiogenic signaling by activation of stem cell factor. PLoS One. 2013; 8(7):e68176. [PubMed: 23861869]
23. Arcangeletti MC, De Conto F, Ferraglia F, Pinardi F, Gatti R, Orlandini G, et al. Human cytomegalovirus proteins PP65 and IEP72 are targeted to distinct compartments in nuclei and nuclear matrices of infected human embryo fibroblasts. J Cell Biochem. 2003; 90(5):1056–67. [PubMed: 14624464]
24. Hemmati HD, Nakano I, Lazareff JA, Masterman-Smith M, Geschwind DH, Bronner-Fraser M, et al. Cancerous stem cells can arise from pediatric brain tumors. Proc Natl Acad Sci U S A. 2003; 100(25):15178–83. [PubMed: 14645703]
25. Jackson EL, Garcia-Verdugo JM, Gil-Perotin S, Roy M, Quinones-Hinojosa A, VandenBerg S, et al. PDGFR alpha-positive B cells are neural stem cells in the adult SVZ that form glioma-like growths in response to increased PDGF signaling. Neuron. 2006; 51(2):187–99. [PubMed: 16846854]
26. Lathia JD, Gallagher J, Heddleston JM, Wang J, Eyler CE, Macswords J, et al. Integrin alpha 6 regulates glioblastoma stem cells. Cell Stem Cell. 2010; 6(5):421–32. [PubMed: 20452317]
27. Ligon KL, Huillard E, Mehta S, Kesari S, Liu H, Alberta JA, et al. Olig2-regulated lineage-restricted pathway controls replication competence in neural stem cells and malignant glioma. Neuron. 2007; 53(4):503–17. [PubMed: 17296553]
28. Castillo JP, Kowalik TF. Human cytomegalovirus immediate early proteins and cell growth control. Gene. 2002; 290(1–2):19–34. [PubMed: 12062798]
29. Gangemi RM, Griffero F, Marubbi D, Perera M, Capra MC, Malatesta P, et al. SOX2 silencing in glioblastoma tumor-initiating cells causes stop of proliferation and loss of tumorigenicity. Stem Cells. 2009; 27(1):40–8. [PubMed: 18948646]
30. Fang X, Yoon JG, Li L, Yu W, Shao J, Hua D, et al. The SOX2 response program in glioblastoma multiforme: an integrated ChIP-seq, expression microarray, and microRNA analysis. BMC Genomics. 2011; 12:11. [PubMed: 21211035]
31. Xu N, Papagiannakopoulos T, Pan G, Thomson JA, Kosik KS. MicroRNA-145 regulates OCT4, SOX2, and KLF4 and represses pluripotency in human embryonic stem cells. Cell. 2009; 137(4): 647–58. [PubMed: 19409607]
32. Kim J, Kwon YJ, Park ES, Sung B, Kim JH, Park CG, et al. Human cytomegalovirus (HCMV) IE1 plays role in resistance to apoptosis with etoposide in cancer cell line by Cdk2 accumulation. Microbiol Immunol. 2003; 47(12):959–67. [PubMed: 14695446]
33. Yu Y, Alwine JC. Human cytomegalovirus major immediate-early proteins and simian virus 40 large T antigen can inhibit apoptosis through activation of the phosphatidylinositide 3′-OH kinase pathway and the cellular kinase Akt. J Virol. 2002; 76(8):3731–8. [PubMed: 11907212]
34. Zhu H, Shen Y, Shenk T. Human cytomegalovirus IE1 and IE2 proteins block apoptosis. J Virol. 1995; 69(12):7960–70. [PubMed: 7494309]
35. Goldmacher VS. vMIA, a viral inhibitor of apoptosis targeting mitochondria. Biochimie. 2002; 84(2–3):177–85. [PubMed: 12022948]

36. Dziurzynski K, Wei J, Qiao W, Hatiboglu MA, Kong LY, Wu A, et al. Glioma-associated cytomegalovirus mediates subversion of the monocyte lineage to a tumor propagating phenotype. Clin Cancer Res. 2011; 17(14):4642–9. [PubMed: 21490182]
37. Wiesner SM, Decker SA, Larson JD, Ericson K, Forster C, Gallardo JL, et al. De novo induction of genetically engineered brain tumors in mice using plasmid DNA. Cancer Res. 2009; 69(2):431–9. [PubMed: 19147555]
38. Price RL, Song J, Bingmer K, Kim TH, Yi JY, Nowicki MO, et al. Cytomegalovirus contributes to glioblastoma in the context of tumor suppressor mutations. Cancer Res. 2013; 73(11):3441–50. [PubMed: 23729642]
39. Temme A, Geiger KD, Wiedemuth R, Conseur K, Pietsch T, Felsberg J, et al. Giant cell glioblastoma is associated with altered aurora b expression and concomitant p53 mutation. J Neuropathol Exp Neurol. 2011; 69(6):632–42. [PubMed: 20467329]
40. Soroceanu L, Akhavan A, Cobbs CS. Platelet-derived growth factor-alpha receptor activation is required for human cytomegalovirus infection. Nature. 2008; 455(7211):391–5. [PubMed: 18701889]
41. Cobbs C, Khan S, Matlaf L, McAllister S, Zider A, Yount G, et al. HCMV glycoprotein B is expressed in primary glioblastomas and enhances growth and invasiveness via PDGFR-alpha activation. Oncotarget. 2014; 5(4):1091–100. [PubMed: 24658280]
42. Slinger E, Maussang D, Schreiber A, Siderius M, Rahbar A, Fraile-Ramos A, et al. HCMV-encoded chemokine receptor US28 mediates proliferative signaling through the IL-6-STAT3 axis. Sci Signal. 2011; 3(133):ra58. [PubMed: 20682912]
43. Mao P, Joshi K, Li J, Kim SH, Li P, Santana-Santos L, et al. Mesenchymal glioma stem cells are maintained by activated glycolytic metabolism involving aldehyde dehydrogenase 1A3. Proc Natl Acad Sci U S A. 2013; 110(21):8644–9. [PubMed: 23650391]
44. Lu KV, Chang JP, Parachoniak CA, Pandika MM, Aghi MK, Meyronet D, et al. VEGF inhibits tumor cell invasion and mesenchymal transition through a MET/VEGFR2 complex. Cancer Cell. 2012; 22(1):21–35. [PubMed: 22789536]
45. Bhat KP, Balasubramaniyan V, Vaillant B, Ezhilarasan R, Hummelink K, Hollingsworth F, et al. Mesenchymal differentiation mediated by NF-kappaB promotes radiation resistance in glioblastoma. Cancer Cell. 2013; 24(3):331–46. [PubMed: 23993863]
46. Mitchell DA, Batich KA, Gunn MD, Huang MN, Sanchez-Perez L, Nair SK, et al. Tetanus toxoid and CCL3 improve dendritic cell vaccines in mice and glioblastoma patients. Nature. 2015; 519(7543):366–9. [PubMed: 25762141]
47. Li RY, Baba S, Kosugi I, Arai Y, Kawasaki H, Shinmura Y, et al. Activation of murine cytomegalovirus immediate-early promoter in cerebral ventricular zone and glial progenitor cells in transgenic mice. Glia. 2001; 35(1):41–52. [PubMed: 11424191]
48. Kosugi I, Shinmura Y, Kawasaki H, Arai Y, Li RY, Baba S, et al. Cytomegalovirus infection of the central nervous system stem cells from mouse embryo: a model for developmental brain disorders induced by cytomegalovirus. Lab Invest. 2000; 80(9):1373–83. [PubMed: 11005206]
49. Schuessler A, Walker DG, Khanna R. Cytomegalovirus as a novel target for immunotherapy of glioblastoma multiforme. Front Oncol. 2014; 4:275. [PubMed: 25340042]

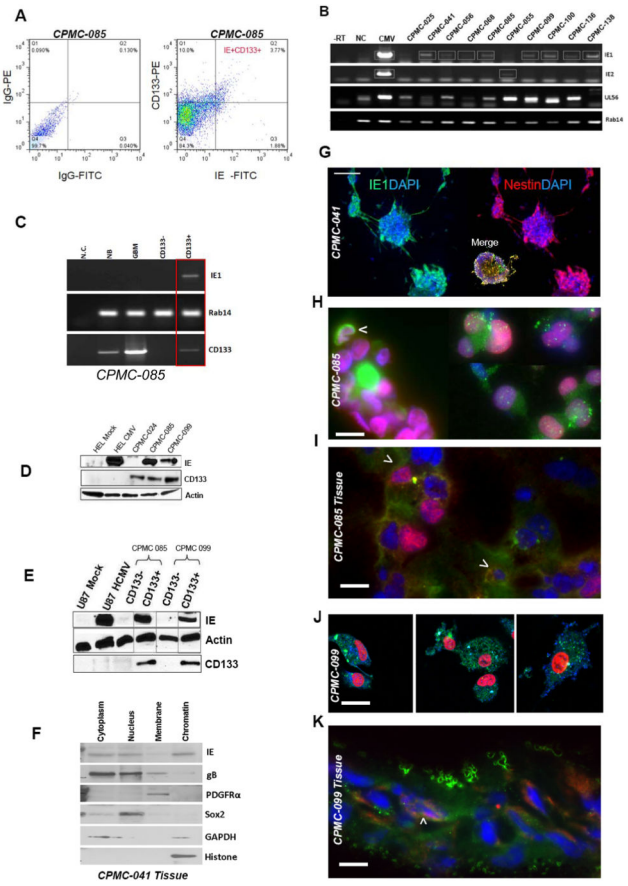

Figure 1. HCMV IE are expressed in human GSC

A. FACS analysis of acutely dissociated GBM cells labeled with control antibodies (left panel) and IE-FITC/CD133-PE (right panel). **B.** RT-PCR detection of HCMV IE1, IE2 and UL56 mRNA in primary human GBM and control samples. Squares designate samples which were confirmed by sequencing. Rab14-control. **C**. RT-PCR detection of IE1 transcript. NC- negative control, NB- uninvolved brain tissue. CD133+/− primary cells isolated from the same specimen. **D–E**. Western blot analysis of primary GBM frozen tissues (**D**) and corresponding CD133+/− cellular fractions (**E**) for HCMV IE. Actin is used as loading control. **F.** Western blot analysis of sub-cellular fractions obtained from CPMC-041 GBM tissue shows localization of viral and cellular proteins, as indicated. **G**. CD133+ neurospheres derived from CPMC-041 stained for IE (green) and Nestin (red); nuclei counterstained with DAPI. Bar=200μm. **H**. CD133+ neurospheres isolated from CPMC-085 GBM sample were processed by immunofluorescence to detect IE (green) and Sox2 (red). Nuclei counterstained with DAPI. Bar= 100μm. **I.** Flash frozen CPMC-085 tissue was processed for double immunofluorescence to detect IE (green) and Sox2 (red). Nuclei counterstained with DAPI. Bar= 100μm. Arrows indicate areas of co-localization between IE and Sox2. **J**. CD133+ cells isolated from CPMC-099 GBM sample were immunostained for IE (green) and Sox2 (red, left and middle panels) or Nestin (red, right panel). Nuclei counterstained with PI. Bar=50μm. **K**. Flash frozen CPMC-099 tissue was

processed for double immunofluorescence for IE (green) and Nestin (red). Nuclei counterstained with DAPI. Bar= 100μm.

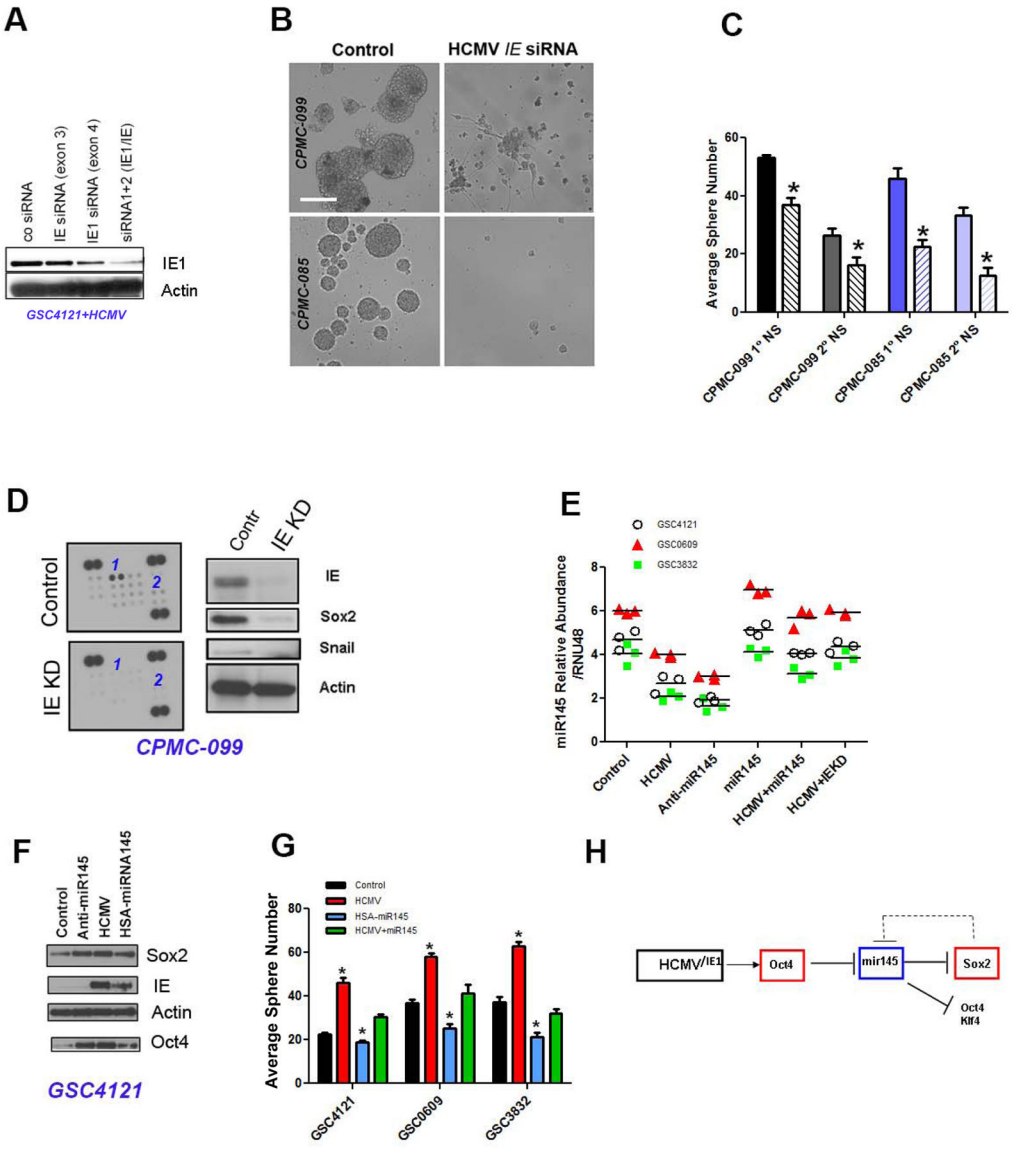

Figure 2. HCMV IE promote self-renewal of GSCs by regulating the miR145-Sox2 axis

A. GSC4121 infected with HCMV (TR, 72h, MOI=1) and treated with non-targeting control siRNA or the combination of IE targeting siRNA duplexes, were analyzed by western blot with the indicated antibodies. **B**. Photomicrographs of CD133+ neurospheres isolated from the indicated GBM samples and treated with control (left panels) or IE siRNA for 72h. Bar=100μm **C**. Primary (1°) and secondary (2°) neurosphere assays +/− IE siRNA. Average neurosphere counts from six wells/condition were used. Bars, SD. ** $p<0.001$, * $p<0.01$, student t-Test. **D**. CPMC-099-derived, CD133+ cell lysates were hybridized to a stem cell antibody array (left panels); western blot validation for the indicated proteins shown in right panels; locations for *1*- Sox2 and *2*-Snail are shown. **E**. Relative abundance of miR-145, normalized to RNU48 levels, measured by Taqman in three GSC lines, treated as indicated. For each GSC line, two way ANOVA tests showed significant differences in HCMV vs Control, HCMV+IEKD or HCMV+miR145 vs HCMV; $p<0.001$ in all comparisons. **F**.

Western blot detection of IE, Sox2, and Oct4 in GSC4121 treated as indicated. **G**. Quantification of sphere formation in 3 GSC lines. Each sample was run in triplicate and the experiment was repeated twice. Bars are SD, * $p<0.002$, student T-test. **H**. Proposed mechanism for HCMV/IE1 regulation of the miR-145-Sox2-Oct4 network.

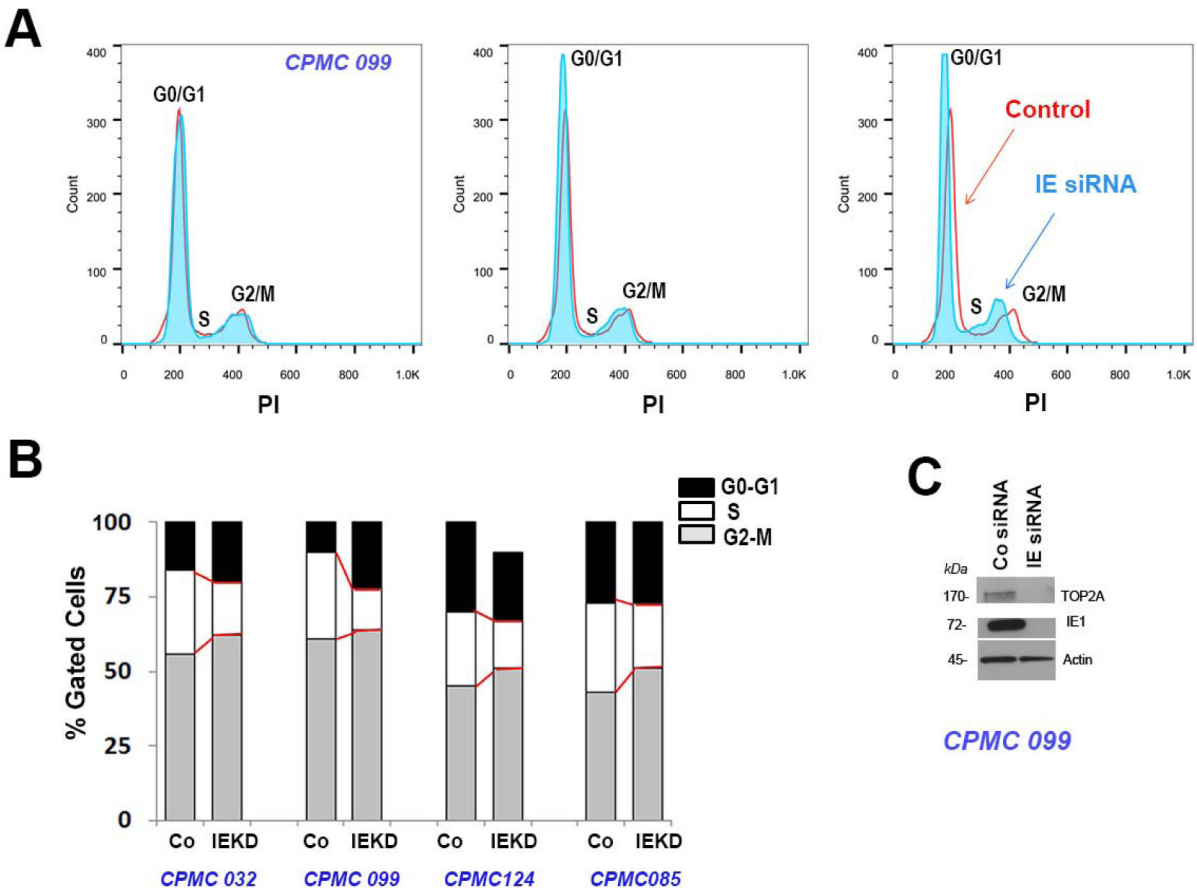

Figure 3. IEKD inhibits S-phase in HCMV positive GSC

A. Cell cycle analyses of endogenously infected, CD133+ GBM cells treated with control siRNA (red line) or IE siRNA (blue). Left panel shows siRNA exon 4 targeting only IE1, middle panel- siRNA exon 3 targeting IE1+IE2, and combined siRNAs are shown in the right panel. PI content was analyzed using FlowJo software. **B**. Bar graph showing cell cycle distribution in four primary GBM samples treated with control or IE siRNA. **C**. Western blot analysis of CD133+ primary GBM cells treated with siRNA as shown (48h).

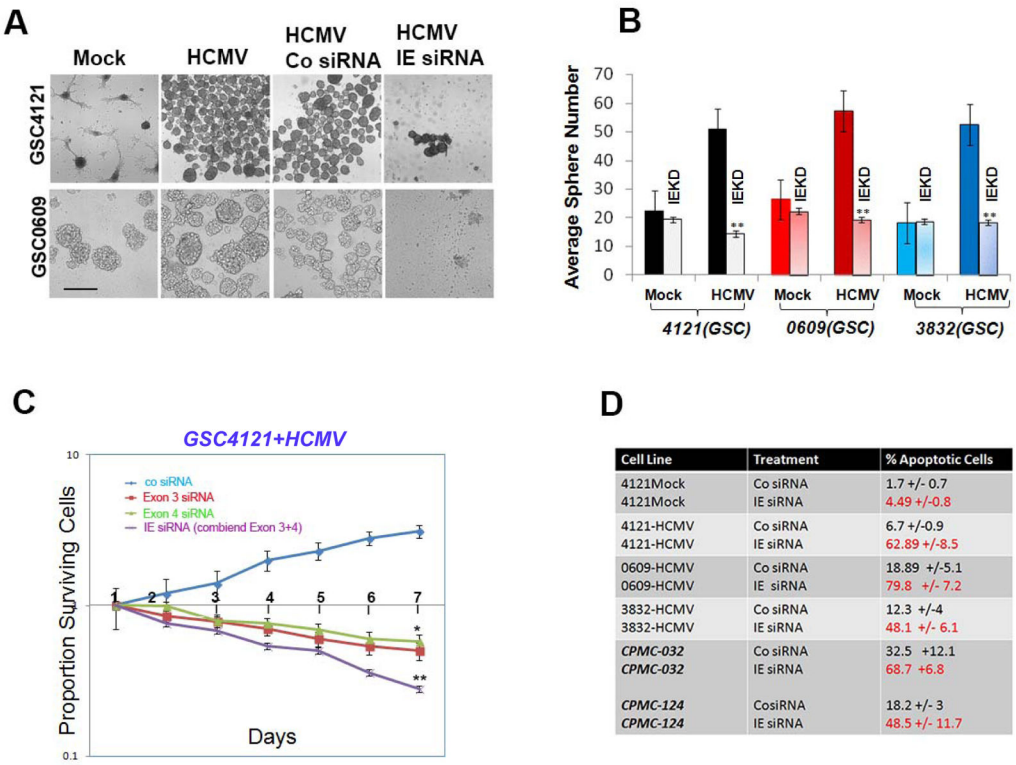

Cell Line	Treatment	% Apoptotic Cells
4121Mock	Co siRNA	1.7 +/- 0.7
4121Mock	IE siRNA	4.49 +/-0.8
4121-HCMV	Co siRNA	6.7 +/-0.9
4121-HCMV	IE siRNA	62.89 +/-8.5
0609-HCMV	Co siRNA	18.89 +/-5.1
0609-HCMV	IE siRNA	79.8 +/- 7.2
3832-HCMV	Co siRNA	12.3 +/-4
3832-HCMV	IE siRNA	48.1 +/- 6.1
CPMC-032	Co siRNA	32.5 +12.1
CPMC-032	IE siRNA	68.7 +6.8
CPMC-124	CosiRNA	18.2 +/- 3
CPMC-124	IE siRNA	48.5 +/- 11.7

Figure 4. IEKD induces apoptosis of HCMV-positive GSC

A. Photomicrographs of HCMV negative GSC4121 and GSC 0609, 72h following mock (left panel) or HCMV (second panel) infection. Cells photographed after treatment with control or IE siRNA (48h) are shown in the third and fourth panels from the left. Each condition was run in triplicate and the experiment was repeated twice. Bar= 50μm. **B**. Quantification of tumorspheres in three GSC lines, treated as indicated. Bars, S.D., ** p<0.002 student T-test. **C.** GSC4121 tested for viability using the Cell Titer Glo assay. Results shown were obtained using 6 wells/condition. Representative data from two repeat experiments. *p<0.01; **p<0.005. **D**. Summary of flow cytometry apoptosis measurements in four GSC samples and two primary GBM cultures treated as indicated. Each sample was run in triplicate. Differences between control and IEKD samples were significant (p<0.02, t-TEST) for all comparisons.

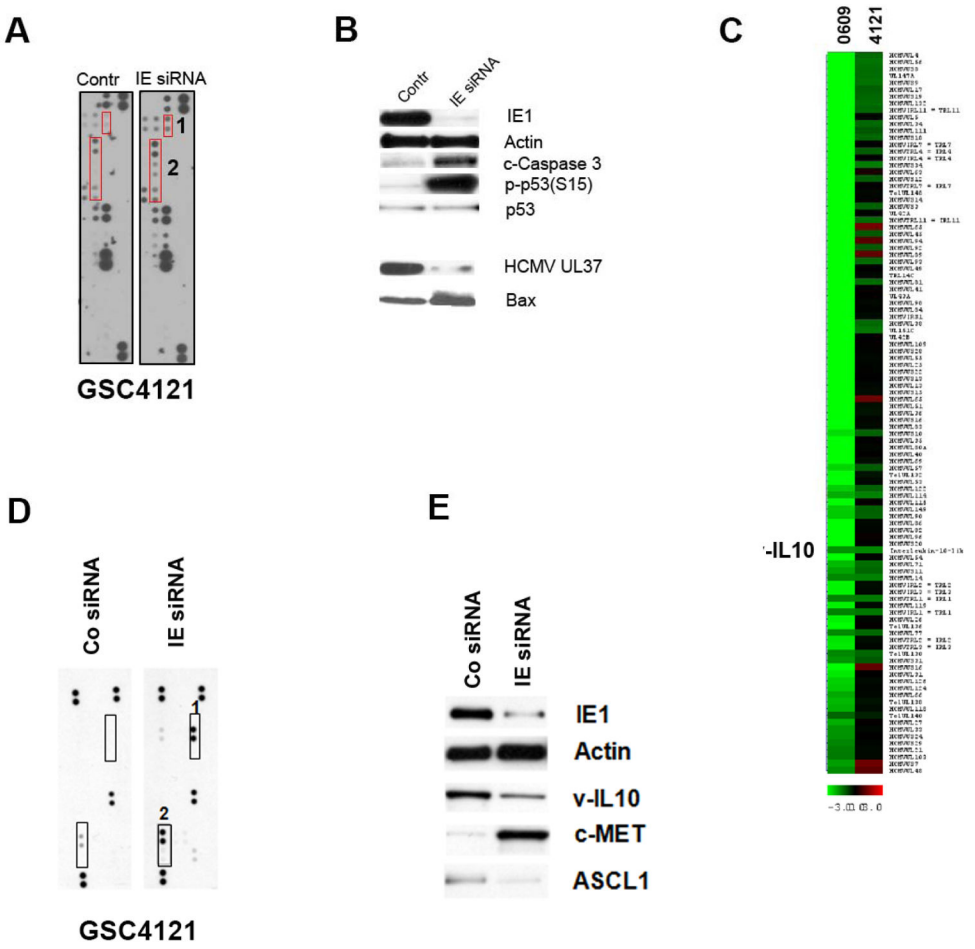

Figure 5. IEKD induces a phenotypic shift in HCMV positive GSC

A. Cell lysates from HCMV-infected GSC4121, treated with control or IE siRNA were hybridized to an apoptosis antibody array. *1*- indicates location of cleaved caspase3 and *2*- location of activated p53 (pS15 and pS20) on the antibody arrays. **B.** Western blot analyses using a portion of the samples arrayed in A with the indicated antibodies. **C**. Hierarchical clustering of HCMV genes significantly downregulated (green) or upregulated (red) by IEKD in two GSC lines. Data was imported to the MEV software and a SAM analysis was performed, using a FDR of zero to determine significance. Duplicate array data was averaged for cluster. **D**. Validation of IEKD- induced changes using a human cytokine antibody array. GSC4121 were used to generate cell lysates hybridized to the arrays spotted with various antibodies. *1* denotes location for Interferon γ. *2* denotes location for CXCL8 (upper) and CXCL10 (lower) on the antibody arrays. **E**. GSC4121 treated with control or IE siRNA were used to generate cell lysates. Viral gene products IE and interleukin-like 10 (v-IL10 or UL111A), and human ASCL1 and c-MET were detected using western blot analyses. Actin is used as a loading control.

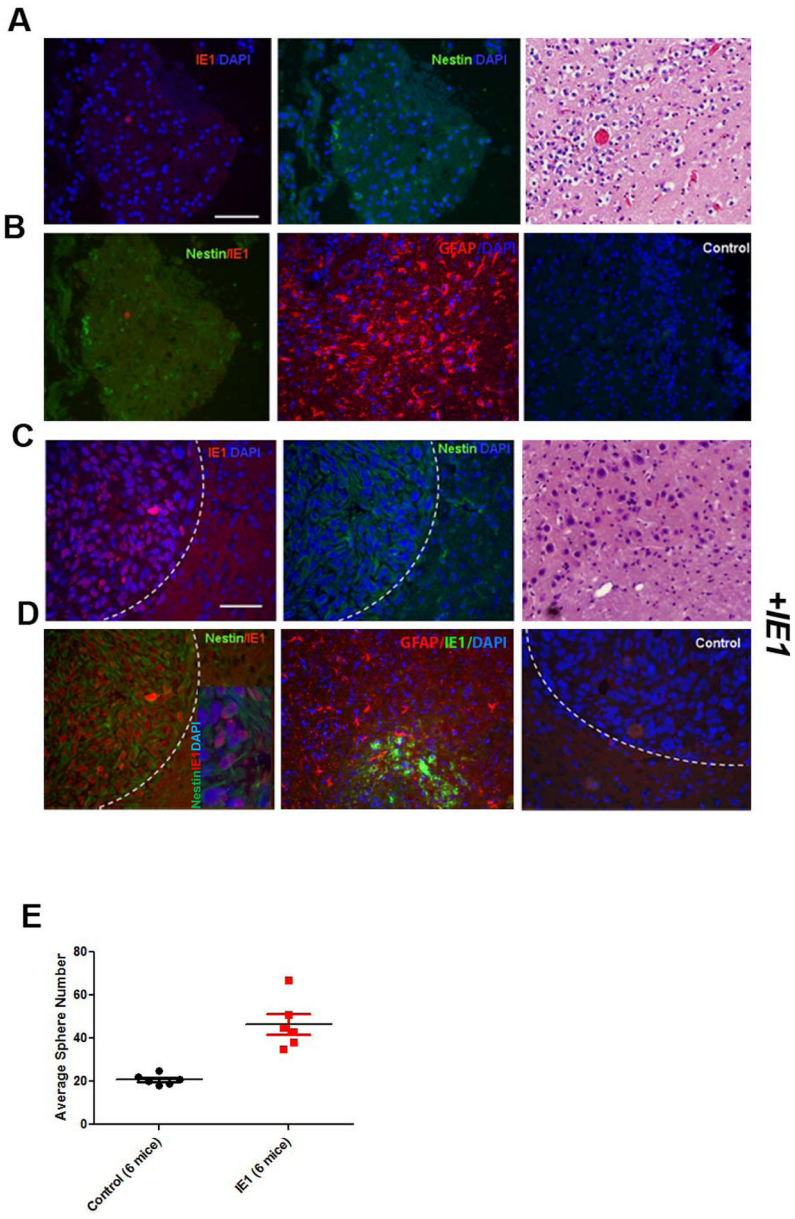

Figure 6. HCMV *IE1* expression augments glioma stem cell phenotype *in vivo*

Immunofluorescence detection of IE1, Nestin, GFAP in representative mouse gliomas induced by *p53*KD/*PDGF/NRasV12* in the absence (**A–B)** or presence (**C–D**) of *IE1*. H&E and control IgG panels are shown for both groups. Bar= 200μm. 5μm sequential sections were stained for IE1, Nestin, and GFAP, as indicated. **D**. Higher magnification photomicrographs of IE/Nestin double labeled tumor section shown in panel insets (C and D). Nuclei counterstained with DAPI. **E**. Freshly dissociated mouse gliomas were assayed for tumorsphere growth. Results show average number of tumorspheres in cultures from six mice/group. $p<0.005$ ANOVA.

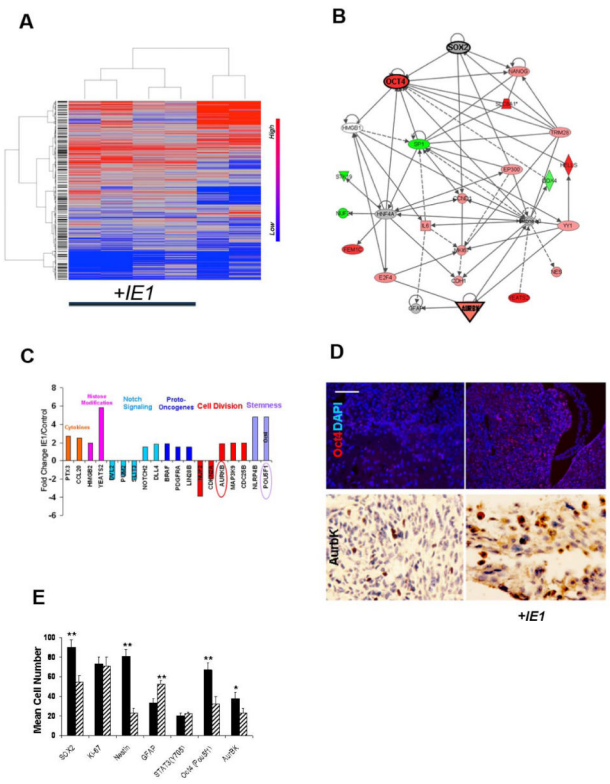

Figure 7. Analysis of spontaneous mouse gliomas +/−IE1

A. Hierarchical clustering (by genes and samples) of 27,368 autosomal gene transcripts in 6 mouse gliomas +/−IE1. Log2 ratios range −0.5 (blue) to + 0.5 (red). **B**. IPA analysis of transcripts significantly upregulated (red) and downregulated (green) in the IE1+ vs control mouse gliomas. **C**. Transcripts significantly different in the IE1+ vs control mouse gliomas are displayed by functional category. **D**. Representative photomicrographs of Oct 4 (upper panels) and Aurora B kinase (lower panels) immunohistochemical detection in IE1+ /− mouse gliomas, bar=150μm. **E.** Four 10X fields from 6 tumors /group were counted for each marker. Solid bars, IE1 + tumors. Mean counts/100 nuclei are shown. ** p<0.003, *p<0.01, student t-Test. Bars, SD.